

Where the Water Really Goes. II. Quantitative
Evaluation of the Net Water Flow
Rate Model for Lithography

by

T. A. Fadner, Fadner Consultants, Oshkosh, WI

ABSTRACT

The recently introduced net water flow rate model for predicting lithographic printing performance relative to ink/water interactions is quantitatively evaluated using operational results from over fifty controlled press tests and nine different inker/dampener configurations. Modeling predictions compare from good to excellent with measured materials utilization and operational acceptability.

The net water flow rate approach is extended in this paper to show the true nature of efficiency in lithographic dampening. The concepts of dampening efficiency are used to explain why water-last and water-first dampening can be equally valid configurations. These principles will allow predicting operational effects caused by dampening for virtually all printing conditions.

BACKGROUND

The first TAGA paper in this two-part set (1) introduced a simple, consistent net water flow rate means for modeling where the water goes during lithographic printing. The method was shown to allow qualitative prediction of relative dampening water input requirements for any lithographic press configuration provided only that efficient dampening water input was used.

In a preceeding TAGA paper (2), experimental values for rates of water and ink inputs to the press, rates of water conveyance to the ink circulation reservoir, and steady state ink reservoir water contents were presented for four of the six keyless lithographic configurations considered in Reference 1. All 56 of the printing tests using configurations A through D of Figure 1 were run at similar speeds, most of them for 20,000 copies or more, all of them at the just above scum

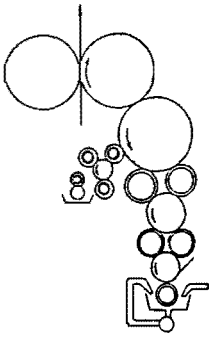


FIG. 1A. WATER-FIRST INKED DAMPENER, LONG INKER

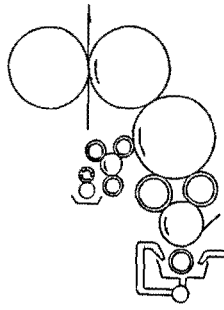


FIG. 1B. WATER-FIRST INKED DAMPENER, SHORT INKER

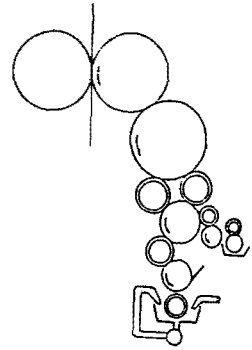


FIG. 1C. INK-TRAIN DAMPENER, LONG INKER

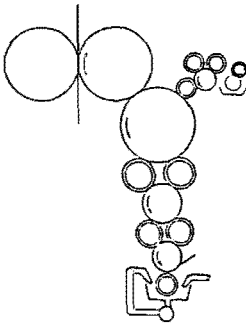


FIG. 1D. WATER-LAST INKED DAMPENER, LONG INKER

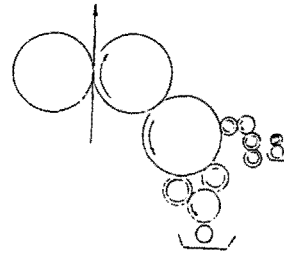


FIG. 1E. WATER-LAST INKED DAMPENER, SHORT INKER

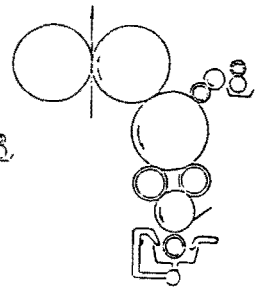


FIG. 1F. WATER-LAST CONVENTIONAL DAMPENER, SHORT INKER

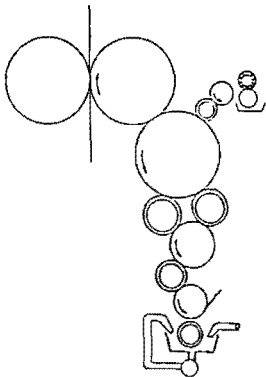


FIG. 1G. WATER-LAST CONVENTIONAL DAMPENER, LONG INKER

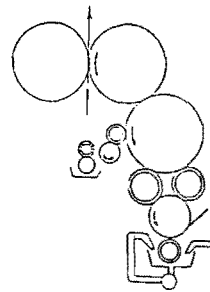


FIG. 1H. WATER-FIRST CONVENTIONAL DAMPENER, SHORT INKER

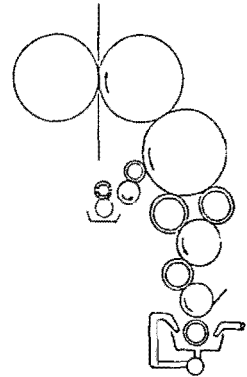


FIG. 1I. WATER-FIRST CONVENTIONAL DAMPENER, LONG INKER

FIG. 1. KEYLESS CONFIGURATIONS CONSIDERED IN THIS RESEARCH

condition. The Figure 1E configuration had been routinely used for exhaustive printing tests prior to when quantitative consumables data were being recorded. The last four of the Figure 1 configurations F, G, H, and I fail to lithograph acceptably in the keyless mode and therefore no quantitative data can be obtained.

Results given in Reference 1 showed that with efficient dampening the rate of water evaporation from each of the press rollers is constant under given operating conditions, that the rate of input of water to the paper is equivalent to the evaporative loss of water from the blanket when operating at the just above scum condition, and that these component output rates are not dependent upon the configurational details of the press system.

Predictions from Reference 1 included that 1) both water-first and water-last dampening should be viable lithographic configurations, despite the preference for water-first systems in the field, 2) both short and long inking trains of rollers can be lithographically efficient but only if efficient input of dampening water is employed, and 3) efficient input of the dampening water should allow predictive modeling of the lithographic process, something inherently not possible with any conventional dampening system, all of which are inefficient. Therefore, predictive modeling had not yet been successfully implemented (3,4,5).

The present paper uses the Reference 2 experimental printing data to quantify comparisons of net water flow rate predictions with actual water use, to define dampening efficiency for the press systems used in this work and to allow extending findings to the practical ramifications for any lithographic press system. The quantitative internal consistency of the model must first be shown.

INTERNAL CONSISTENCY OF THE NET WATER FLOW RATE MODEL

One of the easily measured quantities during keyless printing operations is the water content of the printing fluid (ink plus water) in the circulation system reservoir. At a given steady state

printing condition, this value also corresponds closely to the return ink film water content on the inking transfer rollers to which the metering roller is supplying printing fluid. Sampling is convenient. Automated Karl-Fischer titration provides rapid, accurate water content analysis. Experimental values of water flow rates to the reservoir are readily obtained as the limiting slopes at zero water content derived from plots like Fig. 2 of water content versus copy count (2).

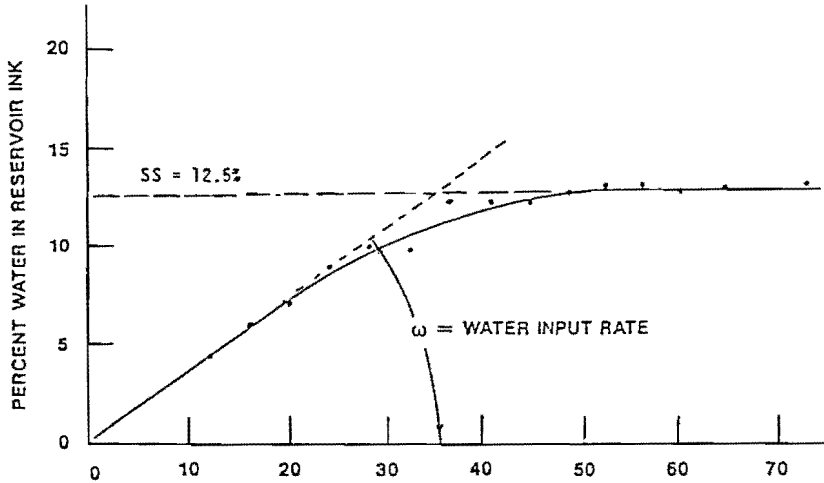


FIG. 2. EXPERIMENTAL DETERMINATION OF WATER FLOW RATES TO INK INPUT RESERVOIR

Unfortunately, the net water flow rate modeling approach by itself does not provide a means to predict water contents in the printing fluid reservoir. Doing so, requires a model of printing fluid transfer action at the metering-roller/transfer-roller nip, such as given in Appendix I, presented in part previously (2).

The water flow rate to the reservoir, w , per press impression is given by Eqn(4) of Appendix I and the proper expressions for the long and short trains of inking rollers considered here are given as Eqns. (5) and (6) below.

$$w = t e \quad (4)$$

$$w_{long} = 0.5 (6-x) [a+(1-a) (1-x)]e \quad (5)$$

$$w_{short} = 0.5 (4-x) [a+(1-a)(1-x)]e \quad (6)$$

in which e is the previously-defined (1) water evaporation rate per impression from a defined portion of a press roller surface under fixed ambient and speed conditions, running at just-above-scum dampening input,

t is the portion of the averaged transfer roller return ink film that is split-off to the metering roller at their mutual nip for subsequent scraping removal,

x is the fractional image content on the plate,

a is the land area fraction (non-celled portion) of the metering roller.

Using the net water flow rate model of Ref.1 and this metering roller return transfer model, Eqns.(5) and (6), values for net water input flow rates were calculated for the first five Fig.1 configurations at three locations 1) the dampening-form/plate nip, 2) the plate/(first) inking-form nip, and 3) the recirculation reservoir. Results are shown in Table I. The corresponding measured values for the first and last of the three press positions are given in Table II for the four configurations that had been experimentally measured.

One measure of a model's internal consistency is whether ratios of predicted relative water flow rates at two different press locations compare favorably with the corresponding experimental water flow rate ratios. Accordingly, Table III lists the predicted and measured ratios of the reservoir water input flow rate to the total rate of dampening water input for each of the four press systems.

The modeling values are within an average of about 8% of actual. This degree of correlation between predicted and actual ratios is excellent, considering the modeling assumptions involved and press test variability that can occur. This result provides strong support for the overall validity of the modeling and the press testing methodologies.

A more revealing assessment of this consistency

TABLE I. CALCULATED RELATIVE WATER FLOW RATES AT THREE PRESS POSITIONS FOR SIX KEYLESS LITHOGRAPHIC PRESS CONFIGURATIONS

<u>Press Configuration</u>	<u>Dampener Location</u>	<u>Inker Type</u>	<u>Average Image Content for Print Tests^a</u>	<u>Metering Roller Land Area for Print Tests^a</u>	<u>Rate of Water Input to Plate^b</u>	<u>Rate of Water Input to Form/Plate Nip^b</u>	<u>Rate of Water Input to Recirculation Reservoir^c</u>
Figure 1A	WF	Long	0.31	0.28	7.5e	7.5e	2.2e
Figure 1B	WF	Short	0.29	0.36	5.5e	5.5e	1.5e
Figure 1C	ITD	Long	0.33	0.36	9.5e ^d	6.0e	2.24e
Figure 1D	WL	Long	0.37	0.28	9.5e	5.5e	2.1e
Figure 1E	WL	Short	0.31 ^f	0.28 ^f	7.5e	3.5e	1.4e

- a. Experimental values from Reference 2 except as indicated.
 b. From Reference 1.
 c. From Equation (5) or (6).
 d. Input in this case is to a rider roller on an inking drum.
 f. Selected average values for calculation purposes.

TABLE II. EXPERIMENTAL WATER FLOW VALUES FOR FOUR KEYLESS LITHOGRAPHIC KEYLESS PRESS CONFIGURATIONS^a

<u>Press Config.</u>	<u>Number of Print Tests</u>	<u>Dampener Location</u>	<u>Inker Type</u>	<u>Rate of Ink Input to Press (ml/imp)^b</u>	<u>Rate of Water Input to Press (ml/imp)</u>	<u>Rate of Water Input to Recirculation Reservoir^c (ml/imp)</u>	<u>Steady-State Water Content Percent in Reservoir^d</u>
Figure 1A	22	WF	Long	0.17	0.24	0.065	12
Figure 1B	7	WF	Short	0.11	0.30	0.094	27
Figure 1C	17	ITD	Long	0.11	0.34	0.075	19
Figure 1D	10	WL	Long	0.24	0.26	0.059	5

- a. All values are from Reference 2.
 b. Measured value assuming specific gravity of 1.0, corrected for comparison to image contents of $x = 0.31$.
 c. By Figure 2 method.
 d. Measured values.

TABLE III. THEORETICAL VERSUS ACTUAL NET WATER FLOW RATE RATIOS FOR LITHOGRAPHIC PRESS CONFIGURATIONS

Config.	Dampener Type	Inker Type	Ratio of Reservoir Water Flow Rate Input To Total Water Input ^a		Percent Difference
			Model	Actual	
Figure 1A	WF	Long	0.29	0.27	7
Figure 1B	WF	Short	0.27	0.31	13
Figure 1C	ITD	Long	0.24	0.22	9
Figure 1D	WL	Long	0.22	0.23	4
Figure 1E	WL	Short	0.19	-	-
Average					8

a. Data from Tables I and II.

is comparison of calculated values of the modeling-defined evaporative constant, e , as determined from the experimentally measured water flow rate values for the four configurations. The Table IV listing reveals good to excellent correlation among six of

TABLE IV. CONSTANCY OF THE LITHOGRAPHIC MODELING WATER EVAPORATION RATE

Configuration	Water Input to the Press			Water Flow Rate to Reservoir		
	Model	Actual ^a	e Value ^b	Model	Actual ^a	e Value ^b
Figure 1A	7.5e	0.24	0.032	2.2e	0.065	0.030
Figure 1B	5.5e	0.30	0.054	1.5e	0.094	0.063
Figure 1C	9.5e	0.34	0.036	2.24e	0.075	0.033
Figure 1D	9.5e	0.26	<u>0.027</u>	2.1e	0.059	<u>0.028</u>
Average ^d			0.032	0.030		

a. In ml/impression.

b. In ml/impression from [column 3/column 2] numerical values.

c. In ml/impression from [column 6/column 5] numerical values.

d. For configurations 1A, 1C and 1D.

the eight calculated e values for three of the four configurations. Reasons for the non-fit of the

Fig. 1B values are presented later in this paper.

The Table IV data show that the overall water evaporation rate for each of the Figs. 1A, 1C and 1D configurations is $e = 0.031 \pm 0.003$ ml/imp. This means that the rate of evaporative water loss from one of the large two-around plate and blanket cylinders of a single-width newspaper-like press configuration when operating at about 25,000 impressions per hour at the just-above-scum condition is 0.031 ml of water per half revolution. This value corresponds to two newspaper pages printed one side. The corresponding average ink throughout is about 0.14 ml (one micron film assumed, two 16" x 22" pages, 30% coverage, unit specific gravity). The water throughput at the plate/inking-form nip exit towards the blanket and paper is about 0.096 ml/imp (3e from Reference 1). For comparison, the total water loss, while printing with each of the four configurations ranged from 0.24 to 0.34 ml/imp (Column 3 of Table IV; from Ref. 2).

SIGNIFICANCE OF WATER FLOW RATE MODELING IN THE SELECTION OF PRINTING PRESS CONFIGURATIONS

Having verified remarkably good correspondence between the flow model and actual water flow rates for 3 of 4 lithographic configurations, it is useful to analyze flow rate predictions more closely. Table V lists predicted continuous water flow rates towards two lithographically significant locations 1) the water-form-roller/plate nip and 2) the first inking-form-roller/plate nip. When choosing between long and short inking trains, the ratios of water input rate to ink film thickness at these locations, columns 6 and 9 of Table V, can be used to estimate relative expectation of adverse ink/water interaction problems. The higher the ratio, the more severe and/or the greater number of problems are to be expected.

Only modest adverse water/ink interactions are predicted for water-last dampening because the water-to-ink ratios of Table V are intermediate in value. This is the quantitative reason why Configuration 1E, with water-last dampening, exhibited good to excellent runnability and printed quality (1,2). This result infers lithographic presses

TABLE V. CALCULATED WATER-INPUT-TO-INK-CONTENT RATIOS AT LITHOGRAPHICALLY SIGNIFICANT PRESS LOCATIONS

Press Configuration	Inker Type	Dampener Type	Values Prior To Dampener-Form/Plate Nip			Values in the Inking-Form/Plate Nip		
			Net Water Flow Rate Towards ^a	Relative Ink Film At Plate ^b	Ratio of Water Input to Ink Film ^c	Net Water Flow Rate Towards ^a	Relative Ink Film ^b	Ratio Water Input to Ink Film ^d
Figure 1A	Long	WF	0.23	2	0.12	0.23	6	0.038
Figure 1B	Short	WF	0.17	2	0.085	0.17	6	0.028
Figure 1C	Long	ITD	0.18	2	0.090 ^e	0.18	6	0.030
Figure 1D	Long	WL	0.29	3	0.097	0.17	6	0.028
Figure 1E	Short	WL	0.23	3	0.078	0.11	6	0.018

- a. In ml/imp from Table I, column 6 or 7 multiplied by $e = 0.031$ ml/imp.
 b. From simplified ink film thickness analysis with no starvation modes.
 c. Column 5 divided by column 4.
 d. Column 8 divided by column 7.
 e. Dampener form = inker form for this configuration.

could be designed water-last at least as often as water-first. They are not.

Of the long inker types, 1A, 1C and 1D, ink-train dampening has lower water-to-ink ratios than water-first dampening and perhaps lower than water-last. In practice, water-last has never been preferred over ink-train dampening in the newspaper field where all three have been used, and ink-train dampening appears to be on its way out.

The water-first long inker configuration, although most often used, is predicted to be the least desirable of these operable keyless configurations.

The anomalies between certain of these modeling derived predictions and common lithographic practices, as well as the significantly higher apparent e value for the water-first short inker configuration, Fig. 1B, must be explained if the present methods are to be entirely consistent. The resolution of these anomalies resides in consideration of dampening efficiency concepts.

DAMPENING EFFICIENCY CONCEPTS IN THE LITHOGRAPHIC PROCESS

All droplets or momentary films of water that appear in the printing press roller system as separate water entities or separate phases, that is, as free water existing outside of the continuous phase ink (printing fluid) films with which we print, excepting the free water in plate non-image areas, are of no value in maintaining lithographic image differentiation. Such water is lithographically redundant, lithographically unnecessary, and, in the extreme, detrimental to ink transfer. It can readily be shown that whenever free water droplets or films appear on ink films they can be frictionally conveyed by an inked system of rollers or by the blanket-paper portion of the press away from the region of the plate (6,7). Whenever free water accumulates on press rollers, it can be misted off or printed out from the press system; that corresponding portion of the total input water fed to the press will not have been lithographically available. The dampening system input will have been

inefficiently utilized. Consequently, the rate of water input to the press system will need to be significantly greater than the amount necessary at the plate for lithographic image differentiation. Lithographic problems will be more severe than inherently necessary. The dampening systems cannot be modeled. As supported throughout this paper, these factors describe virtually all of the extant lithographic dampening systems in the world.

With this basis, the four experimentally-measured configurations can again be compared. The lowest of any configuration's calculated apparent water evaporative value will most closely represent the minimal and lithographically natural water loss per unit area of roller surface. It represents a least-water-required, most efficient, lithographic dampening standard. The other three configurations can be listed according to increasingly greater apparent water evaporation rate values as in column 6 of Table VI. It should be noted that these column 6 values rank the same as the differences between theoretical and measured flow rate ratios of Table III, column 6.

TABLE VI. EXPERIMENTALLY DERIVED EVAPORATIVE WATER FLOW RATES FOR FOUR LITHOGRAPHIC PRESS SYSTEMS

<u>Press Configuration</u>	<u>Dampener Location</u>	<u>Inker Type</u>	<u>Experimentally Derived e Values for Indicated Flow Paths^a</u>		<u>Average of Columns 4 and 5</u>	<u>Normalized e Value</u>
			<u>To Press</u>	<u>To Reservoir</u>		
Figure 1D	WL	Long	0.027	0.028	0.028	1.00
Figure 1A	WF	Long	0.032	0.030	0.031	0.90
Figure 1C	ITD	Long	0.036	0.033	0.035	0.80
Figure 1B	WF	Short	0.054	0.063	0.058	0.48

a. In ml/imp from Table IV.

There is no basis to expect different surface water evaporation rate values for the differing configurations evaluated here. All had spiral brush initial water input, speed at 25,000 imp/hour, reasonably well-controlled temperature and humidity in the pressroom, generically similar dampening solutions and inks. The same press test bed was used excepting the purposeful configurational changes. Accordingly, the normalized apparent e values in

column 7 of Table VI represent relative effectiveness of the four lithographic configurations in the utilization of water being input by the dampener. The normalized e values represent these press systems' relative overall dampening efficiencies.

The importance of the Table VI analysis and the concept of quantitative dampening efficiency can be illustrated using actual printing experiences, with the Fig. 1 configurations. In the first paper of this two-part set, it was qualitatively shown that efficient dampening required the presence of three or more oleophilic/hydrophobic rollers carrying water to the plate, uninterrupted by any hydrophilic rollers (1). Portions of that qualitative relationship are reproduced in Table VII together with the quantitative Table VI data and additional qualitative data obtained while using the Fig. 1 configurations.

TABLE VII. EFFECT OF EFFICIENT DAMPENER DESIGN ON (KEYLESS) LITHOGRAPHIC PRINTING PRESS PERFORMANCE

Press Configuration	Inker Type	Dampener Configuration	Relative Dampening Efficiency ^a	Water Problems Model Rank ^b	No. of Oleophilic Rollers Conveying Water to Plate ^c	Press Performance Evaluation ^d
Figure 1D	Long	Inked, WL	1.00	3	3+	G-E
Figure 1E	Short	Inked, WL	High ^e	1	3+	G-E
Figure 1A	Long	Inked, WF	0.90	5	3+	G-E
Figure 1B	Short	Inked, WF	0.48	2	3+	G-F
Figure 1C	Long	Inked, LTD	0.80	4	3+	G
Figure 1G	Long	Conv., WF	Poor ^{e,f}	>5	1	P-F ^g
Figure 1H	Short	Conv., WF	Poor ^{e,f}	>5	1	P-F ^g
Figure 1F	Short	Conv., WL	Poor ^e	>>5	1	Failure ^h

a. From Table VI except as noted.

b. From Reference 1, Table I. Lowest value is predicted best. See also, columns 6 and 7, Table I.

c. From Reference 1, Table III or from Figure 1, this paper.

d. From Reference 1, Table III except as noted.

e. Author's laboratory observations from numerous printing tests.

f. Includes field test press experience.

g. Field experience including several competitive product withdrawals.

h. Occasional failure in the field.

Although the 1 to 5 rank predictions in Table VII, column 5, do not exactly follow the calculated relative dampening efficiency values, column 4, it is clear that the only acceptable keyless press configurations are those involving an uninterrupted set of three or more oleophilic/hydrophobic rollers for dampening water input. These are designated "inked" in the Dampener Configuration Column.

These results define that the Fig. 1A through

1E systems involve sufficiently efficient dampening input that all of them print acceptably, good or excellent. None of the conventionally dampened press configurations Fig. 1F through 1I were operationally or lithographically acceptable. Relative dampening efficiency concepts correlate especially well in this regard.

PREDICTION OF WATER CONTENTS IN THE INK ON PRESS

The author's modeling method assumed that all press roller surface positions rapidly fill with an amount of water that allows just achieving the natural rate of water evaporation loss from each of the components. Having demonstrated the efficacy of the model, it follows that the steady-state water content in the printing fluid at any press position can be determined from the modeled relative rates of ink and water throughputs at that position.

For example, the relative net rate of water flow to the plate/inking-form nip for the water-first long train configuration, Fig. 1A, reproduced here from Reference 1 modeling as Fig. 3, is $r = 7.5e = 0.23 \text{ ml/imp}$. Although the average ink

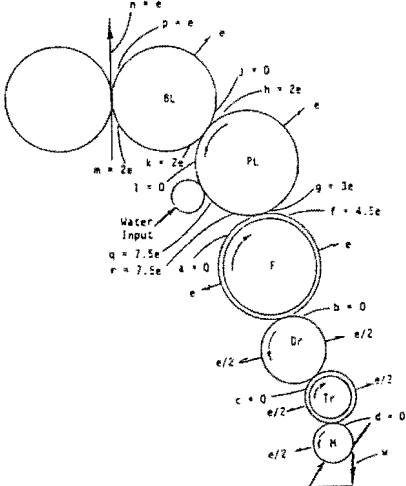


FIGURE 3. NET WATER FLOW RATES FOR EFFICIENTLY-DAMPENED WATER-FIRST LONG-INKER KEYLESS PRESS CONFIGURATION

film thickness in that nip is 6, the continual replenished or active ink film input to the plate/ink form nip in any keyless system corresponds to a printed-out ink film of unit thickness at 100% coverage. The measured rate of ink use for this configuration was 0.17 gm/imp at 31% image content (2). The upper ink layer throughput at the plate/form nip therefore was 0.55 gm/imp (0.17/0.31) or, at unit specific gravity, 0.55 ml/imp. Based on these throughputs, the momentary water content of the uppermost unit thickness printing fluid film at the plate/form nip was 29% $[(100 \times 0.23) / (0.55 + 0.23)]$.*

Table VIII contains predicted water contents at the plate/inking-form nips for the five keyless configurations that were studied. The circulation reservoir water content calculations are given in Appendix II. The measured reservoir water contents are also given in Table VIII. Again, three of the four sets of measured quantities correlate very

TABLE VIII. PREDICTED AND MEASURED WATER CONTENTS
IN INK ON PRESS

<u>Press Configuration</u>	<u>No. of Press Tests</u>	<u>Inker Type</u>	<u>Dampener Type</u>	<u>Predicted Water % in Ink at Plate/Inking-Form Nip</u>	<u>Predicted Steady-State % Water in Reservoir</u>	<u>Measured Steady-State % Water in Reservoir</u>	<u>Rank of Expected Ink/Water Problems</u>
Figure 1A	22	Long	WF, Inked	29	11	12	3
Figure 1B	7	Short	WF, Inked	33	10	27	5
Figure 1C	17	Long	ITD	20	19	19	4
Figure 1D	10	Long	WL, Inked	27	9.3	11.5	2
Figure 1E	Many	Short	WL, Inked	23	0.7	-	1

a. From Appendix II, based on actual water input rate.

b. From Reference 2.

c. Not measured as explained in text.

d. Rank of the Column 6 values. Lowest rank represents least problems.

*Of this water content, 3e must go to the plate and 4.5e back towards the inker. Consequently, the average relative water throughput of the whole ink film at that nip is given approximately by

$$\frac{[(5 \times 4.5e) + (1 \times 7.5e)]}{6} = 0.15 \text{ ml/imp}$$

and the average percent water in the printing fluid at that location is 21% $[(100 \times 0.15) / (0.55 + 0.15)]$.

well with predicted values, Figs. 1A, 1C and 1D, columns 6 and 7. It is therefore likely that the corresponding column 5 predicted plate/form-roller water contents in the ink for these configurations are realistic, ranging from 23 to 33%.

The short-train water-first dampened system, Fig. 1B, was only about 67% efficient. Measured water content was 27% versus a predicted value of 18%. At least one-third of the input water was ineffective in dampening the plate and was conveyed as free water into the inking system, much of which ended up in the circulation reservoir, the rest being misted off or printed out. Notice, again, that the conventionally dampened keyless counterpart, Fig. 1H could not operate acceptably.

One of the interesting predictive results from Table VIII is that the water-last configurations should have lowest water input to the printing fluid reservoir, inferring least water interference problems. Recently, a keyless press product utilizing these principles was offered to the Japanese news-printing market as the Rockwell MLX press (8).

Column 8 of Table VIII ranks the expectation of water problems for the five operable configurations, with the numeral 1 assigned as least severe. These rank values can be derived from water contents at the plate/inking-form nip and/or that at the printing fluid circulation reservoir. It should be noted that the latter also serves as the printing fluid (ink) input location.

REALITIES OF EFFICIENT DAMPENING

Many of the world's keyless lithographic press product candidates have used conventional water-first dampening and short inking trains, such as shown in Fig. 1H. All of these types have failed, as explained herein, due to excess water interference. Others utilized water-first conventional dampening with long inkers, Fig. 1I, resulting in marginal operating and quality acceptance relative to lithographic standards. Keyless inking is not the problem. Products based on any of the Fig. 1 configurations can deliver a smooth uniform overall solid ink film when the dampener is off. The less

than acceptable results show up in Figs. 1F to 1I when the dampener is turned on.

With this well-documented world-wide experience, it is not surprising that the Fig. 1B water-first short inker test configuration of Table VIII ranked lowest of the five operable keyless press configurations. It required the highest dampening water input rate to print at the just-above-scum condition (Table VI). Nevertheless, because of its inked dampening rollers, this configuration ran sufficiently well so that it can be considered as a potential keyless product mode. All attempts with the otherwise similar Fig. 1H configuration, which has conventional dampening, have failed or have operated poorly in the field.

In contrast with this experience, the otherwise strongly correlatable net water flow rate modeling approach predicts that this Fig. 1B configuration should be one of the most trouble-free relative to water. The predicted rank was second best (Table VII). Its performance rank (Table VII) and therefore its dampening efficiency rank of Table VIII were not nearly as good. The discrepancy for this configuration is resolved in the following paragraphs.

Based on efficient dampening concepts, it is safe to assume that input dampening water being forced onto both image and non-image areas of the plate is made available primarily in efficient micron-dimensioned form at the next encountered nip whenever inked rollers dampening water input is used. In this respect, water-last and water-first configurations do not differ. However, in any lithographic configuration, the incoming ink film on the first inking form roller is also continuously forced into contact at its plate nip both with the image areas and with the free-water containing non-image areas of the plate. Free water of finite dimensions can readily be forced from the plate non-image areas onto the form roller ink film as discontinuous films of water. The subsequent net water flow paths towards the ink input system of rollers and back towards the plate involves only one or two fully inked nips at which to remicronize that free water into lithographically useful dimensions (Fig. 1B). Previous reports (1,2) documented

that at least three fully inked roller nips are required to convert an input dampening water film into micron sized particles or clusters within the ink films. This criterion logically must also be operational for free water being forced from the plate non-image areas into the inker portions of a lithographic press. Thus, for any press system to have overall efficient dampening, three or more inked nips are also required in all water flow paths within the inking portion of the press.

None of the conventionally dampened water-first short inker keyless lithographic configurations Fig. 1B tested in the field meet this inked nips criterion within the inker portion of the press. None of this type configuration can match the Reference 1 modeling efficiency predictions nor can they function lithographically as efficient as configurations that meet this criterion. Incorporation of inked rollers in the dampener of the Fig.1B configuration obviated its abject failure but it still performed least well of those judged acceptable.

With this insight, the recirculation reservoir water content modeling prediction of 18% for the Fig. 1B configuration can be corrected. Using only the overall actual water input rate to the press and the new insight features of the model, as shown in Appendix III, the predicted reservoir water content accurately matches the measured value of 27% shown in Table VIII.

REALITIES OF WATER-LAST DAMPENING

Reference to the water-last long-inker configuration, Fig. 1D, will verify that a sufficient number of fully inked roller nips are available within the inker to micronize free water that might be forced onto the inking form rollers. Minimal free-water problems are predicted and few are encountered during corresponding tests of real systems.

The water-last short inker configuration, Fig. 1E, should be reconsidered in view of the water-first model correction just presented. No press materials data exist in this case to compare model

predictions with actual performance. The issues are 1) why is water-last dampening acceptable here whereas conventional water-last dampening is not acceptable, and 2) is the potential for free-water in the inker expected to be a mitigating factor with water-last short inker dampening as it is for water-first.

The important practical evidence is that water input using inked dampener rollers is essential for water-last short inker lithography to be at all operable.

The major expected advantage of the water-last configuration is that the net water input rate to the important inking-form-roller/plate nip will be much lower than with water-first dampening. Also, the required change in water content in the incoming ink as it travels through that nip is much smaller with water-last dampening. An illustration of this is given in Table IX. Derivation of these data is given in Appendix IV.

TABLE IX. WATER CONTENTS AT THE (FIRST) INKING-FORM/PLATE NIP FOR EFFICIENT WF AND WL DAMPENING

Configuration	Water Content of Uppermost Unit Layer of Incoming Ink (ml/imp) ^a	Required Continuous Water Input to Nip from Dampener (ml/imp) ^a	Water Content of Uppermost Unit Ink Film Within the Nip (ml/imp) ^a
WF, Short Inker (Figure 1B)	0.078	0.171	0.269
WL, Short Inker (Figure 1E)	0.078	0.109	0.187

a. Approximately equivalent to volume fraction.

The Table IX predicted values clearly indicate that when the water-last and water-first short inker configurations are equally efficient in micro-nizing any free input water that appears, it is expected that water-last will be more trouble-free than water-first. Water contents at the first form roller/plate nip are 19% and 26% respectively.

The practical measured fact is that the dampener water input required for water-first short inker lithography Fig. 1B is about 28% rather than the predicted 17%, rendering the water-first configuration even less acceptable. The configurational differences are so great that the continually required dampening water input for water-first, column 3 of Table IX is nearly as high as the total instantaneous water content at the plate/form nip for water-last dampening, column 4 of Table IX.

IMPLICATIONS OF NET WATER FLOW RATE MODELING FOR PRACTICAL PRESS OPERATIONS

The concepts presented here are applicable to any lithographic press system, keyless or keyed, provided that a press configuration allowing efficient dampening is used. With this change, scum-to-wash latitude and ink/water balance can be understood and predicted. Water contents at any press location are calculable. The water flow requirements for differing image contents, for differing substrates and for differing press speeds are predictable.

The effects of pressroom printing conditions, such as change in temperature, change in relative humidity, change to or from alcohol-containing dampening solutions, change to or from three, four, or more printing stations are all predictable and generally calculable.

All of these changes have far less drastic effects on ink/water problems, that is on the process of dampening, when using efficient dampening than with conventional inefficient dampening systems. These factors and more will be presented in the third paper of this net water flow modeling series.

CONCLUSIONS

Lithography can readily be conducted under efficient dampening conditions and the fate of the input water can be accurately predicted but not when using today's conventional inefficient dampeners. Efficient dampening corresponds with the least possible water input required for lithographic

image differentiation, therefore to minimal adverse effects when having to use two fluids to carry out the printing process.

The quantitative reliability of the net water input modeling method shown here allows for the first time utilizing press designs and printing materials that optimize the overall lithographic printing process without having to eliminate dampening. It also allows predicting the effects of printing operational changes on the nature and severity of ink/water problems.

Lithography has been demystified.

REFERENCES

1. T. A. Fadner, "Where the Water Really Goes. I. Derivation of a Definitive Model for the Fate of Dampening Water in the Lithographic Printing Process," 1994 TAGA Proc. 459-482.
2. T. A. Fadner, "Prediction of Steady-State Operations in Keyless Lithography," 1990 TAGA Proc., 363-392.
3. U. Lindquist, S. Karttunen and J. Virtanen, "New Model for Offset Lithography," Adv. Print. Sci. Technol. 16, 67-96 (1982).
4. J. MacPhee, "An Engineer's Analysis of the Lithographic Printing Process," 1979 TAGA Proc., 237-277.
5. Y-H. Zang, "A Model for Ink/Water Balance in the Lithographic Process," 1992 TAGA, 426-442.
6. T. A. Fadner, "Fountain Solution Studies. XIV. Role of Isopropanol in Lithography - An Update," 1979 Annual Res. Dept. Report, 121-131, Graphic Arts Technical Foundation, Pgh.PA
7. T. A. Fadner, "Surface Chemistry Control in Lithography," Colloids and Surfaces in Reprographic Technology, ACS Symp. Series 200, M. Hair and M.D. Croucher, ed., 1982, 347-357.
8. L. Bain, "The Influence of Technology on Lithographic Pressroom Productivity," Critical Trends, Res. Eng. Council, Jan. 1994.

APPENDIX I. WATER TRANSFER INTO THE PRINTING
FLUID RECIRCULATION RESERVOIR OF A CELLED
METERING ROLLER KEYLESS LITHOGRAPHIC PRESS

A previous reference (2) illustrates the averaged relative printing fluid film thickness values near the metering roller for a typical scraped celled metering roller keyless lithographic press that is operating with printing plate image content x . The metering roller input surface has a zero transferable ink-film thickness since the ink is below the surface in cells. The return printing fluid film on the transfer roller has a relative volume of $(6-x)$ when printing out an ink film of unity. The printing fluid film of interest, t , is that continually transferred from the transfer roller to the metering roller surface due to printing fluid film splitting at the exit of the metering roller/transfer-roller nip. It is this transferred return film that is subsequently scraped by the doctor blade into the reservoir.

The fraction, f , of the celled metering roller surface available for splitting of the return transfer roller printing fluid film is given by Eqn. (1).

$$f = [a + (1-a)(1-x)] \quad (1)$$

where a = land area fraction of the metering roller that supports the doctor blade. This portion of the metering roller always participates in return film splitting, independent of image content,

$(1-a)$ = area fraction of the metering roller surface containing replacement printing fluid in cells with $x = 1.0$ being the amount of ink available for transfer to the transfer roller, thereby being able to replenish any amount 0 to x of the unit film thickness of ink that was printed out, and

$(1-x)$ = the non-image area fraction of the printing plate. This quantity also represents the averaged portion of the total metering roller celled area $(1-a)$ that does not need to deliver ink to the transfer roller when printing at image content x . That portion acts as metering roller "land" surface area and therefore participates in return ink film splitting.

Assuming a 50/50 printing fluid film split, the printing fluid film thickness, t , on the return side of the metering roller for the long inker of Fig. 1A is then given by Eqn. (2):

$$\begin{aligned} t &= 0.5 (6-x) f \\ &= 0.5 (6-x) [a + (1-a)(1-x)] \end{aligned} \quad (2)$$

and for the short inker of Fig. 1B, by Eqn. (3):

$$t = 0.5 (4-x) [a + (1-a)(1-x)] \quad (3)$$

In the preceding paper it was shown that the expected net water flow rate at the return side of the transfer roller corresponded to the quantity e . This value accounts for subsequent evaporative losses $e/2$ from each of the two small rollers as shown in Figs. 1A and 1B. As discussed elsewhere in this paper, only the uppermost layer of the return ink film at relative thickness equal to $(4-x)$ or $(6-x)$ for short and long inkers respectively, is involved in this evaporation. Most of the return film has a steady-state water content of e . During a sufficiently long run, it is expected that the maximum circulation reservoir water content will also reach a steady-state content of e . The input to the reservoir is therefore given by Eqn. (4):

$$w = t e \quad (4)$$

APPENDIX II. CALCULATION OF RESERVOIR WATER CONTENTS FROM RELATIVE WATER AND INK FLOW RATES FOR TABLE IX.

1. Configuration Figure 1a: Water-first, Inked Dampener, Long Inker.

The continuous net water input rate to the plate/inking-form nip is $7.5e = 0.23$ ml/imp. The measured ink throughput was 0.17 gm/imp at 31% image content. The ink throughput to the plate at unit specific gravity was 0.55 ml/imp ($0.17/0.31$). The predicted average water content in the continuously throughput ink at that nip is 29% [$(100 \times 0.23)/(0.55 + 0.23)$].

Of the $7.5e$ water input tending to go to all portions of the press, $4.5e$ is lost by evaporation from the inker loss path. The highest net water input value that the ink entering the recirculation reservoir can have is $(7.5e - 4.5e) = 3e = 0.093$ ml/imp. Since the average ink throughput is the same at all press locations, the predicted reservoir steady-state

water is directly proportional to the net water input at the location of interest, in this case the value is 11% $[(0.093/0.23) \times 29]$.

2. Configuration Figure 1A with High Water Input Rate (p23 of text).

The continuous net water input rate to the plate/inking form nip is $12.5e = 0.39$ ml/imp. The measured ink throughput at 31% image content was 0.17 gm/imp or at unit specific gravity and unit film thickness 0.55 ml/imp. The predicted water content in the continuously throughput ink at that nip is 41% $[(100 \times 0.39)/(0.55 + 0.39)]$.

Of the 12.5e water input tending to go to all portions of the press, 4.5e is lost by evaporation from the inker. The highest net water input value that ink entering the recirculation reservoir can have is $(12.5e - 4.5e) = 8e = 0.25$ ml/imp. Since the average ink throughput is the same at all press locations, the predicted reservoir steady-state water content is 26% $[(0.25/0.39) \times 41]$.

3. Configuration Figure 1B: Water-first Inked Dampener, Short Inker.

The continuous net water input rate to the plate/inking-form nip is $5.5e = 0.17$ ml/imp. From Reference 2, the continuous ink throughput was 0.10 gm/imp at 29% image content, which gives a 100% image content ink throughput to the plate/form nip of 0.34 ml/imp $(0.10/0.29$ at unit specific gravity). The predicted average water content in the continuously throughput ink at that nip is 33% $[(100 \times 0.17)/(0.17 + 0.34)]$.

Of the 5.5e water input tending to go to all portions of the press, 2.5e is lost by evaporation from the inker. The highest net water input value that the ink entering the recirculation reservoir can have is $(5.5e - 2.5e) = 3e = 0.093$ ml/imp. Since the average ink throughput at this location is the same as at all press locations, the predicted reservoir steady-state water content is 18% $[(0.093/0.17) \times 33]$.

4. Configuration Figure 1C; Ink-Train Dampening, Long Inker.

The continuous net water input rate to the transfer-roller/inking-form nip is $9.5e = 0.29$ ml/imp. From Reference 2 the continuous ink throughput was 0.12 gm/imp at 33% image

content, which results in a 100% ink throughput to the plate/form nip of 0.36 ml/imp (0.12/0.33, at unit specific gravity). The predicted average water content in the continuously throughput ink at that nip is 45% $[(100 \times 0.29)/(0.36 + 0.29)]$.

Of the 9.5e water input tending to go to all portions of the press, evaporative loss in the inker loss path is 5.5e. The highest water input value that the ink entering the recirculation reservoir can have is $(9.5e - 5.5e) = 4.0e = 0.12$ ml/imp. The predicted recirculation reservoir water content is 19% $[(0.12/0.29) \times 45]$.

5. Configuration Figure 1D; Water-last Inked Dampening, Long Inker.

The continuous net water input rate towards the plate/blanket nip is 9.5e = 0.29 ml/imp. The continuous ink throughput from Reference 2 was 0.29 gm/imp at 37% image content. At unit specific gravity, this corresponds to 0.78 ml/imp throughput at the nip (0.29/0.37). The water content at the nip then is 27% $[(100 \times 0.29)/(0.29 + 0.78)]$.

Of the 9.5e water input tending towards the inker loss path, 6.5e is lost by evaporation from the plate and inker. The highest water input value that ink entering the recirculation system can have is $(9.5e - 6.5e) = 3e = 0.093$ ml/imp. The predicted reservoir water content is 8.7% $[(0.093/0.29) \times 27]$.

6. Configuration Figure 1F; Water-last Inked Dampening, Short Inker.

The continuous net water input rate to the plate/blanket nip is 7.5e = 0.23 ml/imp. For this never-measured configuration, the ink throughput is assumed identical to that for Figure 1D, 0.78 ml/imp. The predicted average water content in the continuously throughput ink at that nip is 23% $[(100 \times 0.23)/(0.78 + 0.23)]$.

Of the 7.5e water input tending continuously to go to all portions of the press, 4.5e is lost by evaporation from the inker. The highest water input value that the ink entering the recirculation reservoir can have is $(7.5e - 4.5e) = 3e = 0.093$ ml/imp. The predicted reservoir water content is 9.3% $[(0.093/0.23) \times 23]$.

APPENDIX III.

The actual water input requirement for the Figure 1B configuration was 0.30 ml/imp (Table II), whereas the minimal requirement based on modeling is 0.17 ml/imp (from Tables I and IV, $5.5e \times 0.031$). The 0.30 ml/imp input value corresponds to $9.9e$ ($0.30/0.031$).

At the inking form/plate nip the continual water throughput is $9.9e$. Of this, $3e$ must go towards the plate-blanket-paper path, leaving $6.9e$ to fill the ink on the inker rollers and in the reservoir. Of the continual throughput relative ink film of 6 at the form/blanket nip, the uppermost layer (1/6th) must carry $9.9e$ at maximum ink throughput, that is, for image content $x = 1.0$. The lower portion will carry a maximum steady-state water content equivalent to $6.9e$. Consequently, the expected average water throughput at the plate/form nip is given by

$$\frac{9.9e + (6.9e \times 5)}{6} = 0.23 \text{ ml/imp.}$$

The measured press ink throughput was 0.10 gm/imp and at unit specific gravity is 0.10 ml/imp. For the actual image content of $x = 0.31$ (Ref. 2), the ink throughput at this nip was 0.33 ml/imp ($0.10/0.31$).

The average percent water relative to the total fluid present is then

$$w_p = (100 \times 0.23)/(0.23 + 0.33) = 41\%$$

At the reservoir, the equivalent ink film of 6 contains the following quantity of continuous water input

$$\frac{6.9e + 5(6.9e - 2.5e)}{6} = 0.15 \text{ ml/imp.}$$

Since the ink throughput is the same everywhere in keyless lithography, the expected reservoir water content is

$$\frac{0.15}{0.23} \times 41\% = 27\%$$

This more accurate predicted value correlates well with the simpler estimates of Appendix II part 2 and with the measured value.

APPENDIX IV

WF, SHORT INKER. The modeling required input to the form/plate nip, from Ref. 1, is 0.17 ml/imp (5.5e). Of this 0.093 ml/imp (3e) goes into the blanket-paper path, never transferring to the inker. Thus at steady state, the upper, evaporatively-active unit layer of the four-unit-layer input ink film carries 0.078 ml/imp (0.17 - 0.093).

The required 0.17 ml/imp continuous water input fills all layers of the ink film to a quantity equal to this rate within 10 to 100 impressions or so. Subsequently, the lower three layers of the average four unit thick ink film continually carry 0.17 ml/imp.

The average water content of the incoming ink film to the plate on the form roller is 0.15 ml/imp from $[0.078 + (3 \times 0.17)]/4$. The average water content of the whole ink film at the nip exit is $[0.078 + 0.17 + (3 \times 0.17)]/4$ or 0.19 ml/imp.

WL, SHORT INKER. Required water input from Ref. 1 is 0.11 ml/imp (3.5e). Of this 0.031 ml/imp (e) goes into the plate path. At steady state, the evaporatively active uppermost unit layer of the four unit layer input ink film carries 0.078 ml/imp (0.11 - 0.031).

The required 0.11 ml/imp continuous input permanently fills the lower three unit ink film layers to that water content.

The average ink film water content on the form roller is $[0.078 + (3 \times 0.11)]/4$ or 0.10 ml/imp. The average ink film water content on the form roller is $[0.078 + 0.11 + (3 \times 0.11)]/4$ or 0.13 ml/imp.